Journal of Biomedical Optics

SPIEDigitalLibrary.org/jbo

Reflectance imaging of the human retina at 810 nm does not suffice to optimize the parameters of hydrodynamic rebalancing laser treatment

Filippo Piffaretti
Jean-Pierre Ballini
Roberto Perotti
Matthieu Zellweger
Edoardo Vezzola
Michel Sickenberg
Georges Wagnières

SPIE

Reflectance imaging of the human retina at 810 nm does not suffice to optimize the parameters of hydrodynamic rebalancing laser treatment

Filippo Piffaretti,[a] Jean-Pierre Ballini,[a] Roberto Perotti,[b] Matthieu Zellweger,[a] Edoardo Vezzola,[b] Michel Sickenberg,[c] and Georges Wagnières[a]
[a]Swiss Federal Institute of Technology, Medical Photonics Group, SB-ISIC, Station 6, 1015 Lausanne (EPFL), Switzerland
[b]Save Sight Foundation, Via Golgi 4, 25087 Salò, Italy
[c]Save Sight Foundation, Av. d'Ouchy 14, 1006 Lausanne, Switzerland

Abstract. The hydrodynamic rebalancing laser (HRL) procedure is an ophthalmic therapy based on the administration of subthreshold infrared (810 nm) laser light to selected areas on the retina to treat various retina diseases. Heterogeneities of tissue response are observed, including undesired retinal damages. Variations of tissue absorbance were hypothesized to cause this uneven response. Irradiation parameters (diameter = 100 μm; power = 1 W; irradiation time: 50 to 200 ms), location and tissue response were studied in 16 patients (20 eyes, 2535 laser spots) to discover any correlation between tissue response and normalized fundus reflectance at 810 nm. The results demonstrate a complex relationship between some pathologies and occurrences of retinal damage, but no clear correlation. One possible reason is that the resolution of reflectance images is insufficient to see "small" (40 μm or less) absorption centers, particularly deep-seated ones. Additionally, tissue parameters other than variations of the fundus optical absorption influence heat diffusion and temperature increases. Monitoring or individualizing the light dose in HRL therapy, or any similar infrared diode laser-based therapy will require more sophisticated technologies, including imaging the retina's reflectance with an improved resolution, as well as refined methods to detect complex correlations between retinal damage and specific pathologies. [DOI: 10.1117/1.JBO.17.11.116027]

Keywords: hydrodynamic rebalancing laser; optical nerve head; choroidal neovascularization; infrared laser therapy; age-related macular degeneration; reflectance; retina; 810 nm.

Paper 12435 received Jul. 10, 2012; revised manuscript received Oct. 16, 2012; accepted for publication Oct. 17, 2012; published online Nov. 22, 2012.

1 Introduction

Laser light has become a standard tool for the treatment and diagnostic of various conditions affecting the eye including the retina.[1–8] Many retinal conditions such as age-related macular degeneration (AMD),[2,9] diabetic retinopathy,[10] retinal tears,[11,12] macular edema,[13,14] and intra ocular tumors[15,16] can be more or less efficiently treated by delivering suitable laser light. In certain cases (e.g., retinal tears) the laser is just used to perform a mechanical welding of the retinal layers. Other laser therapies include the treatment of secondary cataracts with pulsed YAG lasers, the treatment of glaucoma, and the correction of refractive errors. In some other pathologies (e.g., diabetic retinopathy), the periphery of the retina is denatured, to preserve central vision. In many cases, the mechanisms that lead to improvement of the vision are not yet fully understood (decreased demand for, or increased supply of, oxygen) and are the objects of ongoing research. Despite the observed treatment efficacy, a deeper understanding of the mechanism of the treatments is still needed for further optimization.

The regimes and types of laser–tissue interactions commonly used in these retinal treatments are either photochemical or photothermal. Photochemical reactions take place, for example, during the treatment of exudative AMD by photodynamic therapy (PDT).[17–19] Photothermal reactions are, on the other hand, the main interaction modality during pan-retinal photocoagulation (PRP),[20–23] which is used to treat diabetic retinopathy, etc. Photothermal regimes and more particularly photocoagulation can cause undesired modifications of the irradiated tissue, among which are retinal burns. If such burns are induced in the neuronal layers, they can produce a whitish lesion significantly increasing light scattering, and may result in a permanent local scotoma in the patient's field of view.

Even though retinal burns are still the endpoint for different suprathreshold laser photocoagulation therapies,[24] it was shown that clinical efficacy is not always related (e.g., in AMD management) to the extent or appearance of those tissue modifications.[25–29] Several new irradiation protocols in ophthalmology, known as "subthreshold protocols" which also rely on somewhat different laser sources, have been developed. They aim at a controlled and limited temperature increase of the neuronal retinal layers and seek to avoid retinal burns.[14,22,27,30–32]

The temperature increase can be restricted to the irradiated tissues if the laser irradiation period is kept much shorter than the tissue's thermal relaxation time τ_T (obtained by equating the characteristic optical penetration depth, L, to the time-dependent characteristic thermal penetration depth, $z_T(t) = \sqrt{4kt}$, where k is the tissue thermal diffusivity of the tissue. Thus $\tau_T = L^2/4k$). For example, several groups[33–35] have studied what is sometimes designated as "micropulse laser thermotherapy," whereby repetitive short laser pulses

Address all correspondence to: Georges Wagnières, Medical Photonics Group, Swiss Federal Institute of Technology, SB-ISIC, Station 6, 1015 Lausanne, Switzerland. Tel: +41216933120; Fax: +41216935110; E-mail: georges.wagnieres@epfl.ch.

0091-3286/2012/$25.00 © 2012 SPIE

(Nd-YLF laser 527 nm, 1.7 μs) at a large irradiance (0.2 to 0.4 MW/cm^2) are administered to selectively treat the retinal pigmented epithelium (RPE). Even though the highly absorbing RPE cells are directly in contact with the photoreceptors and the neuronal layers, irradiation times of the order of a few μs allow to photomechanically destroy them while sparing the nearby photoreceptors. Analysis of the results obtained with these methods indicates an amelioration of the clinical outcome and a reduction of side effects.[33,35]

Another example of such subthreshold therapies is transpupillary thermotherapy (TTT). It was evaluated for the treatment of subfoveal choroidal neovascularisation (CNV) in AMD,[16,36–41] as well as nonexudative AMD[2,42–44] and other pathologies (circumscribed choroidal hemangioma, serous detachment of the neurosensory retina secondary to chronic central serous chorioretinopathy).[45,46] For this treatment, a near-infrared (810 nm) diode laser was chosen because of its high tissue penetration and the relatively weak absorption of melanin and macular pigments at this wavelength. These characteristics allow the targeting of deeper structures, typically 100 to 300 μm below the photoreceptors and the neuronal layers of the retina. As a consequence, this preserves the photoreceptors and the neuronal layers of the retina, even during long irradiation periods, thanks to the limited heat diffusion from the deep-seated absorbing centers. Long (usually 60 s) laser pulses with small irradiance (2 to 8 W/cm^2) are used to significantly increase the temperature in the neighborhood of the submacular CNV.[47–49] This heating induces vessel damage and thrombosis to the pathological neovascularisation. Moreover, the weak absorption of hemoglobin at this wavelength allows for macular irradiation even in the presence of retinal and subretinal hemorrhage, which once again helps to preserve the neuronal layers.

The treatment of the retina by hydrodynamic rebalancing laser (HRL) therapy[50,51] is yet another approach presenting similarities with TTT. HRL therapy is based on the administration of 70 to 200 subthreshold laser spots (at 810 nm) in selected locations of the retina that are not vital for sight, thus excluding the optic nerve and the macula. Direct treatment of the macula, as is the case in TTT, would not be safe in the case of HRL (Fig. 1).

The HRL therapy is performed with a conventional slit-lamp and a Goldmann contact lens,[52] which gives access to a large field of view and helps to avoid excessive movement of the patient's eye. HRL makes use of a continuous-wave (CW) near infrared laser (810 nm), with power levels from 0.4 to 1.0 W, a constant spot diameter of 100 μm on the retina, and irradiation pulses ranging from 50 to 200 ms.[50]

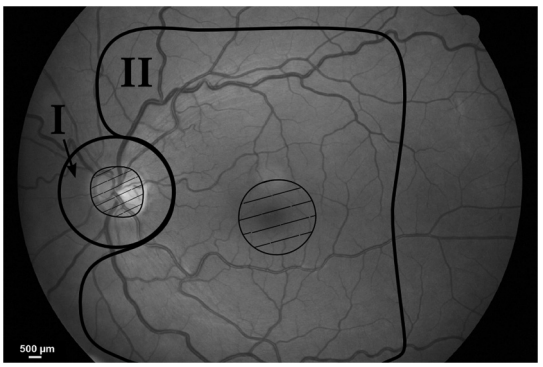

Fig. 1 Subdivision of the retina in two treatment zones. The treated zones, I and II, are delimited with thick lines. The macular and ONH zones, circled and hatched with thin lines, are to be avoided.

Clinical observations suggest that the best clinical outcome is achieved by administering laser pulses near the upper limit of the subthreshold regime.[53] Historically the developments of HRL treatment modalities are based on the clinical observation by Walter,[54] who noticed significant modifications of the temporal border of the optic nerve head (ONH). These abnormalities were present in several patients affected by different pathologies. This led to the working hypothesis that numerous macular diseases have a pathological origin associated with the ONH's disk leakage of extravascular fluids. Vezzola then proposed a new 810 nm laser treatment to restore the hydrodynamic balance within the posterior pole.[55]

Although the mechanistic processes at the base of HRL therapy are not well understood, a reasonable hypothesis seems that the laser acts in such a manner that it reduces some of the typical effects induced by aging and/or ocular hypertension.[56–60] Indeed, both these processes produce modifications at the level of the lamina cribrosa, resulting in a diminished retinal venous outflow due to progressive, central retinal venous (CRV) compression. The increased resistance to venous blood outflow probably leads to an accumulation of excess fluids (blood plasma and serum), which leak at the level of the ONH and then move to the macula and the surrounding tissue.[51,60–65] These abnormal leaks and the resulting fluid accumulation at the choroid–retina interface are thought to be at the origin of various maculopathies. This hypothesis is also supported by work performed by Sickenberg et al.,[66] who studied the initial stages of fluorescein angiography performed on patients with chorioretinal neovascularisation (wet AMD). Fluorescence angiography with fluorescein and a scanning laser ophthalmoscope (SLO) demonstrated a small but measurable ONH's leakage in some of the patients. It was not at all clear whether these leaks had a physiological or pathological cause, but these observations suggested that the leakage was related to a rupture of the hemato-retinal barrier or to direct leaking of cerebrospinal fluids into the retinal space.

Several thousands patients have been treated by HRL therapy as of February 2012, with a good safety profile. These treatments were associated with "unpredictable" retinal burns in 2% to 3% of the laser spots. Small hemorrhages were observed less frequently, in 0.02% of the laser spots. These side effects were categorized as "unpredictable" because their occurrence could not be correlated with the effective laser parameters or the average fundus absorbance as perceived by the clinician. Therefore, a reasonable hypothesis was to attribute these side effects to a heterogeneous distribution of "deep-seated optical absorbing centers" in the eye's fundus.[67,68] This hypothesis was supported by the fact that firing the HRL laser on large pigmented structures of the choroid (choroidal naevi) frequently led to such side effects. Additionally, both small deep-seated absorbing centers of the eye's fundus and choroidal pigmented structures are frequently difficult to localize, even under near-infrared fundus inspection.

Large variations in the optical properties of the retina, in the visible and/or the near-infrared, have been demonstrated by other groups.[15,69–72] Additionally, the relevance of near-infrared reflectance for the detection of some choroidal abnormalities[73] or fundus structure[74] has also been reported.

Therefore, the present study aims at investigating if the observed side effects of HRL are correlated to the presence

of highly absorbing structures in the fundus tissue. A logical strategy to prevent the occurrence of the described side effects and to improve the safety of the HRL treatment as a consequence would then consist in reducing the laser spots irradiation time or the laser irradiance at locations of the retina presenting a strong absorption. Direct *in vivo* measurements of the eye's fundus absorption are not possible, which is why clinical diagnosis, including inspection of the retina, makes use of fundus reflectometry. Thus, measuring the fundus reflectance, in particular when executed at the wavelength of the treatment laser, could possibly help to evaluate spatial variations of the fundus absorption, in an approach similar to that used by de Graaf et al.,[75] Ludwig et al.,[76] and Naess et al.[77] This strategy was applied in the present study to determine if the tissue response during HRL treatment is correlated with fundus reflectance. A preliminary study[55] demonstrated that it is feasible to correlate retina reflectance in infrared (IR) and overtreatment. This present study aims at drawing statistically significant conclusions in the clinical settings: if the correlation turns out to be strong, it will open the door to optimize laser parameters for the treatment. If it is weak or partial, it will show that pigmentation does not play a dominant role in the cascade of events leading to (overtreatment) by HRL and that other parameters should be considered to design a complete method to optimize laser treatment parameters such as blood flow, retinal thickness, presence of edema, etc.

2 Materials and Methods

2.1 *Study Design*

The study took place in April and June 2008 and all measurements were done in Salò, Italy. Sixteen patients (for a total of 20 eyes treated by HRL) took part in this study, with ages ranging from 22 to 78 years (mean age $= 50.75 \pm 16.12$ years). All these patients gave their informed consent to be part of the study. Their enrollment only involved taking two additional images and recording the laser parameters, in addition to the "standard" HRL treatment. In the "standard" procedure, three fundus images are taken to plan the HRL treatment: a color picture, a red-free picture (obtained with a red-free filter described as the B1 curve on Fig. 2 fitted on the ophthalmoscope to better evidence blood vessels as per standard ophthalmoscopic practice), and a fluorescein angiogram.

HRL treatment elicits a small percentage of "unpredictable" responses from fundus tissue, even when the laser's irradiation parameters are kept constant. Our working hypothesis links this heterogeneity in the tissue reaction to the pigmentation density and its distribution in the eye's fundus. Thus, our study focused on the comparison of sites of (infrequent) retinal burns with unburned tissue nearby as a function of the local tissue absorbance—as "deduced" from its reflectance—measured at the laser spot location. Two additional fundus images were taken for that purpose as follows: one near-infrared (810 nm) reflectance image just before the HRL session, to measure the fundus reflectance, and one white-light image just after each administered laser spot, to record the spot location [a video camera (Optronics®, CS-450) was focused on the eye fundus during the treatment—see Instrumentation section].

Whenever a laser pulse was administered by the clinician, the corresponding video image, showing the precise laser spot position, was captured and recorded. Simultaneously, the laser power and irradiation time used were recorded in order to draw up an accurate cartography of the HRL treatment. The map of the laser spot positions and irradiation parameters was then superimposed on the initial infrared reflectance (IRR) fundus image.

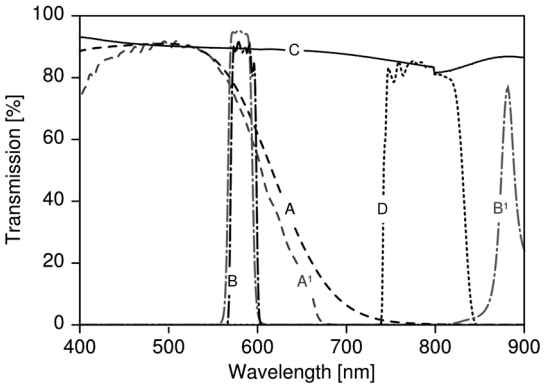

Fig. 2 Optical transmission of the standard filters (A^1, B^1), and of the replacement and additional filters (A, B, C, D), used in the ophthalmoscope. A^1: Original Canon® EOS-D1 CCD filter; B^1: Original redfree filter; A: X-Nite CCD filter, used for balanced color images; B: Replacement redfree filter; C: New CCD filter, used for IRR images; D: IRR image excitation filter.

During the treatment, the clinician was asked to assess whether the laser–tissue interaction created or did not create a visible retinal "burn." Each laser spot was thus characterized and tagged with the clinician's observation, allowing us to establish whether a correlation existed between the local fundus reflectance and the laser tissue response.

2.2 *HRL Treatment*

HRL treatments are routinely performed in several private practices and up to June 2010, more than 5000 patients have been treated.[78] A typical HRL treatment session consists of a series of 100 to 200 laser shots, with the laser beam focused on the retinal pigmented epithelium (RPE). According to the clinical observations, treatment efficacy is maximal when using laser pulses at the upper limit of the subthreshold regime (data not published). During the treatment, shots aimed at the macula and the optic nerve head are carefully avoided. The laser treatment is administered via a solid state, CW, ophthalmologic laser source (810 nm) (Optikon 2000 S.p.a., Elios, $\lambda = 810$ nm), coupled to a standard slit lamp (Takagi®, SM-70N).

The irradiation parameters are chosen by the clinician, depending on the apparent fundus pigmentation and clarity of the ocular media of each patient. To evaluate these irradiation parameters, a test laser pulse is shot on a temporal, peripheral zone of the eye fundus (a similar procedure is also used during PRP to find laser parameters adequate for creating mild retinal burns).

In this study, the laser spot diameter on the retina was kept constant to 100 μm for all the treated patients and the laser power was set to 1 W—except in one particular patient where the power was lowered to 0.4 W. This was at the clinician's demand, in view of keeping these laser spots at the limit of the subthreshold regime (the specific patient was affected by a severe myopic condition). The maximum irradiation time was chosen by the clinician and set between 50 and 200 ms. However, the laser firing system allowed the clinician to terminate irradiation before this preset, thus making it possible to

"personalize" and modulate every single laser spot. The precise duration of the laser irradiation was described in the Instrumentation section.

In addition, the retina was divided into two zones (Fig. 1), in view of grouping the fired laser spots in relatively homogeneous retinal zones: zone I was defined to be an annular region around the optic nerve head; zone II was delineated by the inferior and superior retinal arcades. During the study, the laser spot diameter (100 μm) and the radiant power (1 W; 125 W/mm^2) were kept constant, except for a dozen of laser spots fired in zone II of a single, strongly myopic eye, where the radiant power was lowered to 0.4 W (50 W/mm^2): this was done at the clinician's demand, in view of keeping these laser spots at the limit of the subthreshold regime, as detailed in the HRL Treatment section.

2.3 *Instrumentation*

2.3.1 *Acquisition of the IR reflectance images*

The setup used to record IR reflectance images relies on standard commercial apparatus, with minor modifications. It consists of a digital camera (Canon®, EOS-1D) attached to an ophthalmoscope (Canon®, CF-60UVi). The filters in the camera and the ophthalmoscope were replaced as described below (see Fig. 2).

The charge-coupled device (CCD) filter of the camera was changed to improve its sensitivity in the near-infrared. Thus the band-pass filter used for visible wavelengths (A1), which was normally mounted in front of the CCD, was replaced by a clear glass window (C). The ophthalmoscope's filter set was modified to match the enhanced spectral sensibility of the camera. Thus the standard green band-pass filter (B1) for removing parasitic transmission bands in the IR range was replaced with an interferometric filter (B) (Chroma®, HQ585-30X) to enable the acquisition of the diagnostic "red-free" images with minimal noise. A visible-wavelengths band-pass filter (A), (LDP LCC®, X-NiteCC1), was used to acquire white-light balanced color images. Finally a near-infrared band-pass filter (D) (Chroma®, HQ790/95X) was used to filter out the flash light when acquiring the fundus IRR images. Note that the band-pass filter for the acquisition of the fluorescein angiograms was not modified. These minor modifications did not affect the effective resolution of the diagnostic system, which was found to be about 40 μm for the standard color pictures.

2.3.2 *HRL treatment: data acquisition and processing*

The setup is schematically shown in Fig. 3. The clinician (1) administered the HRL treatment to the patient's eye (3) using a standard slit-lamp (2) (Takagi®, SM-70N). To fire a laser pulse, the clinician pressed on the laser driving pedal switch (4). Additionally, the clinician was instructed to press a second pedal switch (4b) whenever he perceived an increased reflectance, i.e., a whitening of the treated spot, thus tagging the laser spot as a retinal burn. A digital video camera (Optronics®, CS-450) was coupled to the slit-lamp (2) to record the position of each laser spot. Simultaneously the effective irradiance period (tL) and the laser power (PL) were measured with a calibrated fast photodiode (OSRAM®, BPX61, typical switching time 20 ns) integrated in the medical laser (5) (Optikon 2000 S.p.a., Elios, $\lambda = 810$ nm). The photodiode signal was digitized and analyzed with a data acquisition board (Acquitek, F-91300 Massy) integrated to the personal computer [PC (6)].

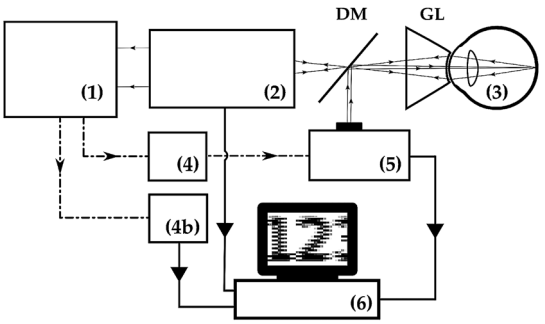

Fig. 3 Schematic representation of the experimental HRL treatment setup, used in this study: at the beginning of the session, the clinician (1), examines the patient's eye (3) through the slit-lamp (2), which incorporates also the video camera; the clinician then adjusts the treatment laser (5), setting the desired power and maximum irradiation time; to apply one laser pulse, he/she presses on the pedal switch (4), which (i) starts the laser, whose beam is directed on the eye fundus by the dichroic mirror (DM) and the Goldman lens (GL) and (ii) triggers the recording of the corresponding video image and laser parameters in the PC (6); the clinician releases pedal switch (4) to stop the irradiation; if he observes the formation of a retinal burn, he tags the corresponding laser spot, by pressing pedal switch (4b).

Recording of the HRL treatment information (laser position, irradiation parameters, and clinician's observations) was triggered by the fast photodiode, every time the clinician pressed on the laser driving pedal switch (4). Dashed lines with arrows in Fig. 3 represent the driving signals. A self-written software drove the acquisition of the data from the three different sources as shown by the solid lines with arrows in Fig. 3.

The fast photodiode was calibrated with a standard power sensor (Coherent®, FieldMaster–GS LM-2) to give the effectively delivered power (PL) and the irradiation time (TL) measured at full width half maximum (FWHM) of each laser spot. The image of the laser treatment site, acquired with the video camera attached to the slit-lamp, was recorded immediately at the beginning of the laser irradiation. The time needed for acquiring this image and transferring it to the PC was less than 40 ms (average file size $\approx$1 MB), which was shorter than the shortest irradiation period. Recording of all the measured HRL treatment parameters was done in less than 400 ms. This duration was compatible with the $\approx$2 Hz laser firing frequency typically used in the HRL laser treatment protocol.

2.3.3 *Data superimposition/registration*

A semiautomatic procedure was used to record the information and superimpose the slit-lamp pictures with the IRR images. In a first, automated step, the slit-lamp images, which reported the laser spot locations, were transformed, reoriented, and scaled to the images taken with the ophthalmoscope. In a second, manual step, the slit-lamp images reporting the HRL treatment position were registered with the corresponding IRR image. The superimposition process relied on the presence of at least a partial, characteristic vascular pattern in the slit-lamp images, which had to be found and identified in the wide field ophthalmoscopic IRR pictures. Both images were then manually registered, in a two-step process: (i) with the help of a dedicated registration software (ImageJ®, Turboreg[79]), assisting the manual registration, the IRR images were registered and overlayed with "redfree" fundus images (Fig. 4); (ii) exploiting the retinal vascular net present in the "redfree" fundus images, the slit-lamp

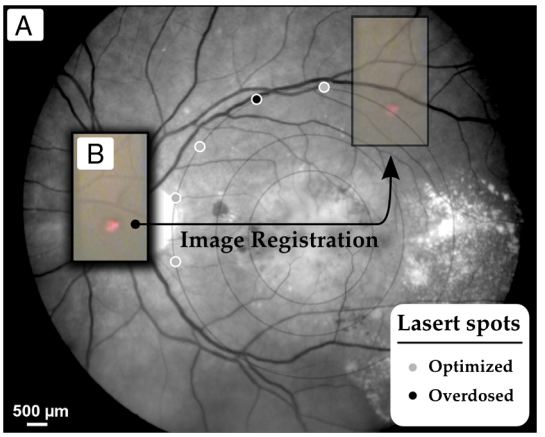

Fig. 4 Image registration: HRL irradiation parameters and spot position (B), superimposition on the "red-free" image (A).

images were manually registered to create a precise HRL cartography on the IRR images. According to this software's specifications, the precision of these computer-assisted registrations is in the subpixel range. In our case we estimated it to be on the order of 50 μm on the retina.

All the laser shots tagged as "having caused retinal burn" (i.e., about two to four per treated eye) were registered, plus a few "subthreshold" laser spots around them i.e., some two to five "subthreshold" shots, located within 2 mm of each "burn-causing" shot. Data analysis started with the slit-lamp images reporting the retinal position of these nearby subthreshold laser spots, selected for comparison purposes as their proximity reduces the influence of other tissular parameters on the optical absorbance, including choroidal blood flow, accumulated chorio-retinal fluids, and chorio-retinal thickness.

3 Eye Fundus Infrared Reflectance Image Processing

Quantitative measurements of the fundus reflectance rely on the standardization and calibration of the fundus illumination. Even though the parameters of the flash used for acquiring the IRR images were kept constant for all patients, this did not result in a stable and homogeneous illumination of the fundus. The excitation heterogeneity was due, among others, to variations in the patients' pupil diameter, the optical properties of their eye media, and the entrance angle of the excitation light, rather than to flash fluctuations. Therefore, the IRR images were normalized to the flash's image pattern, using a simple image processing method: for any specific case, the reflectance image was filtered with a low-pass filter (>1 lp/mm on the retina) to extract the flash excitation pattern. The IRR image was then normalized by dividing the image itself by the flash excitation pattern, resulting in a normalized IRR image, corrected for illumination heterogeneity, over the whole image (Fig. 5).

Such normalized images efficiently emphasize variations in local IR reflectance—at the price of the loss of information on the absolute local reflectance. Despite this shortcoming, detecting these variations in the fundus reflectance (i.e., in its absorbance) made it possible to investigate the assumed correlation between laser parameters, tissue properties, and clinical outcome.

4 Results

Sixteen patients (20 eyes) with good, visible vascular pattern (needed for the overlayering procedure) were treated by HRL in April and June 2008. A total of 2535 laser spots were placed in 20 retinas, causing 67 retinal burns (2.64%). No hemorrhage occurred.

The 20 eyes were undergoing HRL treatment for various conditions and subdivided accordingly in six pathology-specific groups: Glaucoma (seven eyes), Papillary atrophy (four eyes), Age-related macular degeneration (four eyes), Retinitis pigmentosa (three eyes), Myopic retinopathy (one eye), and Diabetic retinopathy (one eye). From the point of view of the ergonomics and adaptability of the measurements, the minor modifications brought to the standard medical device (required for image acquisition and laser data capture) did not significantly influence the medical practice working habits (the increase treatment time was about ≈10%), in spite of the need to acquire two additional images. In fact, thanks to the useful property of these images to highlight the presence of large, deep-seated absorbing structures such as choroidal naevi, their acquisition became part of the clinical routine.

The results are presented in Fig. 6, which shows the analyzed laser spots independently from the patient's eye pathology. Occurrences of retinal burns are shown by triangular marks (△) while subthreshold spots are marked with filled dots (•). The two samples (retinal burns versus subthreshold spots) are not statistically significantly different ($p = 0.45$), which can be deduced from the graph and is well aligned with our observations and conclusions.

Similarly, Fig. 7 shows the results taking into account the treated eyes' pathologies. Specific symbols are assigned to each pathology. Retinal burns are distinguished from subthreshold laser spots through the use of a filled symbol.

Our results do not show a clear correlation between local IR reflectance and propensity to retinal burns. This can be observed by examining groups of iso-energetic laser spots (which lie along horizontal lines in our scatterplots). Retinal burns appear

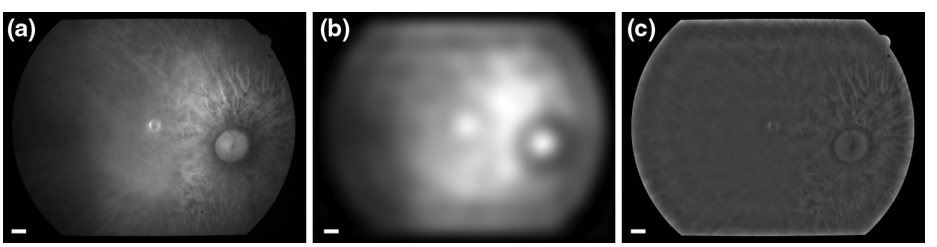

Fig. 5 Correction of IR eye fundus images for the heterogeneity of the ophthalmoscope excitation light: (a) Raw IR fundus image at 810 nm; (b) Intensity pattern of the 810 nm excitation light flash; (c) Corrected IR fundus image obtained by dividing image (a) by image (b). White bar 1 mm on the retina.

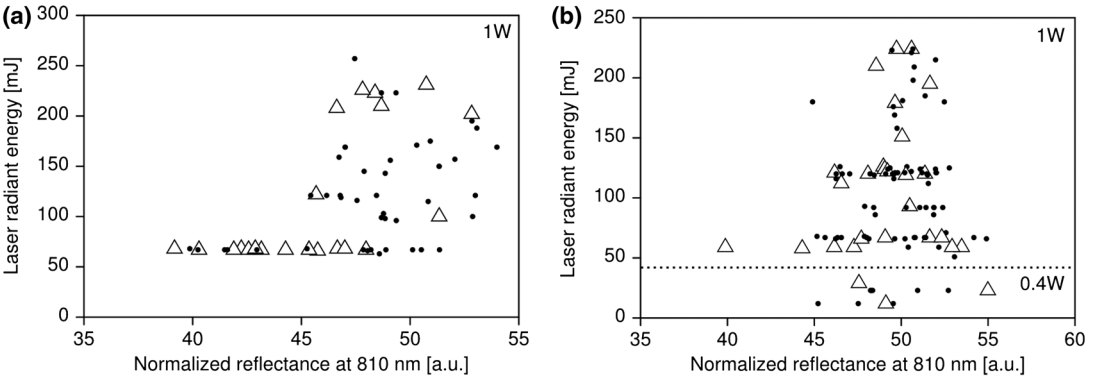

Fig. 6 Scatterplots showing the occurrence of retinal burns (△) as a function of the local, normalized IR reflectance and the effective laser energy administered. Subthreshold laser spots are shown as filled dots (•). (a) Retinal zone I and (b) Retinal zone II.

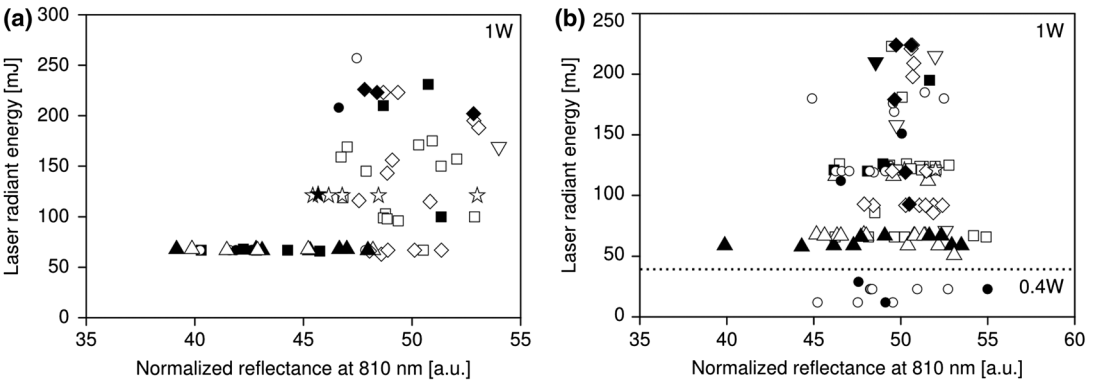

Fig. 7 Scatterplots of all treated eyes, according to retinal zone and eye pathology. Empty symbols correspond to subthreshold laser spots. Filled symbols correspond to retinal burns. ☆: Myopic retinopathy; △: Retinitis pigmentosa; ◇: Atrophic age-related macular degeneration; □: Papillary atrophy; ▽: Diabetic retinopaty; ○: Glaucoma. (a) Zone I and (b) Zone II.

to be randomly distributed between low-reflectance spots (i.e., high absorbance) and high-reflectance spots (i.e., weak absorbance), suggesting that the local normalized reflectance is not an adequate parameter to predict the occurrence of retinal burns.

Furthermore, by analyzing the results according to laser shot radiant energy (along the vertical axis in Fig. 6), considerable variations in the energy of retinal burn-tagged laser spots can be noted. Similarly, in Fig. 7, it is of interest to note that as expected, pathology-specific clustering along the vertical axis is observed: patients affected by retinitis pigmentosa, for example, were found to be grouped in the lower part of the graph. This is likely to be related to a high absolute value of their fundus' absorbance, which is not measurable with our approach as we have only measured the normalized reflectance.

5 Discussion

Reflectance imaging is a reference method for analyzing eye fundus. Since the first quantitative studies published in 1950, a growing interest[68] in quantitative measurements paralleled the adoption of new, laser-based diagnostic technologies [scanning laser ophthalmoscope (SLO); optical coherence tomography (OCT)].[80,81]

Most of these investigations assessed the retinal oxygen contents or the macular pigmentation density in different pathologies,[68,82–85] while a small number of studies focused on the optimization of the irradiation parameters in thermal retinal therapies. Thus, in the framework of PRP, the treated spot's quantitative reflectance was monitored to adapt the irradiation time: it was found that the very important changes in tissue reflectance induced by retinal burns could be used to drive this thermal therapy and control the extent of tissue modifications.[86–89]

To our knowledge, no study investigated the local near-infrared reflectance to optimize a thermal, IR laser therapy. The main advantages of near IR radiation reside in deeper tissue penetration compared to shorter wavelengths and improved transmission through blood and retinal edema.[90,91] The light fraction absorbed in the RPE is about 30% to 35% at 810 nm, compared to approximately 70% at 532 nm.[92–94] This explains why higher IR radiant energy is needed to produce retinal burns (20 kJ/cm^2 at 810 nm versus 1 J/cm^2 at 532 nm). Thus, the pigmentation and the amount of hemoglobin within the choroid, which are linked to choroidal thickness, will probably play a significant role in the absorption process. In such a situation with no dominating absorbing structures, modeling the thermal process causing the retinal burns is difficult. The most plausible hypothesis is that the IR radiant energy is primarily absorbed by the choroidal melanocytes and by the RPE; the heat generated at these two main absorbing centers then diffuses to the neuroretinal layers, where it causes the retinal burns.[15,94–97] It follows that homogenizing the outcome of IR thermal therapies on the basis of the tissue's absorbance is not trivial, as the absence of correlation found in our study could be the consequence of several effects.

Our results do not show a complete lack of correlation. For instance, all the measurements on eyes suffering from retinitis pigmentosa are grouped in the lower part of Fig. 7 (vertical axis values of 50 to 100). On the other hand, the laser shots that

resulted in burns in those patients are poorly separated from those that did not result in burns. This hints at a correlation more complex than our hypothesis presumed. Patients with retinitis pigmentosa suffer from vascular changes, leading to the destruction of RPE cells and migration of melanin to shallower depths, thus changing the depth at which the absorption of near-IR photons will occur. Furthermore, these patients tend to suffer from dryness of the retina, which means that heat may take more time to dissipate than in healthy patients. Both elements may explain why the measurements on eyes with this condition show a grouping that is unlikely due to chance, but is one parameter that characterizes the tendency of retina to undergo burns, and is too complex for our approach to detect fully.

An interesting feature of our data is that some eyes tend to suffer from retinal burns, while some others seldom do (data not shown). This suggests a cascade of events leading to retinal burns that our approach did not demonstrate. This also shows that there is a set of anatomo-physiological characteristics of some eyes that gives them a tendency to suffer retinal burns. Likely, these characteristics are more complex than our approach can detect, and the method needs to be refined further to detect them.

It is worth remembering that this therapy relies on a protocol at the upper limit of the "subthreshold" regime, which implies that all the laser spots administered were very close to the radiant energy required to generate a retinal burn. We should also note that (1) our absorbance measurements are integrated over all the eye media and fundus layers and (2) the longitudinal distribution of the absorbing centers was not measured. Therefore, small changes in eye tissues properties or in the administered energy could lead to these apparently heterogeneous results.

Other parameters may influence the tissue's response to HRL treatment: small, involuntary eye movements during the spot's duration (maximum 200 ms) can probably be neglected: the short irradiation time, the almost painless nature of the treatment, the nearly invisible laser beam, and the Goldmann contact lens are all elements that support this assumption.[52,90,98] Lund[99] studied the impact of small-scale ocular motion on retinal thermal laser therapies. The relief factor (defined as the ratio between the retinal thermal threshold damage in a moving eye and in a theoretical stationary eye) will decrease if during the treatment the patient's eye movement are dampened, and it depended on the irradiation time; it was calculated to be $\approx$10% for an irradiation of 200 ms. As these evaluations were made in the framework of an He-Ne laser therapy (633 nm), it follows that, for the more spatially diffuse tissue absorption during IR therapy, this relief factor should be further reduced.

Laser spot focus changes, caused by the clinician's aiming errors, are probably also of limited relevance for our study. Although the small numerical aperture of the human eye could induce a notable reduction in irradiance (up to a factor three when a longitudinal error of 400 μm is assumed), adjusting the laser spot focus when using a standard slit-lamp is easy, and intra-therapy laser spot focus variations are probably minimal. Moreover, weak absorption and strong scattering in RPE and choroidal tissues further reduce the effect of this parameter.

One possible reason for the inconclusive correlation evidenced by our results is that the geometrical resolution of the reflectance images may not be sufficient to see "small" absorption centers such as melanosomes. If the absorption centers on the fundus are small compared to the resolution of our imaging setup, they may go unnoticed until a laser spot happens to be fired on them. This could explain why we observe no correlation, but observe some undesired retinal burns. If so, overcoming this obstacle would require further refinement of our method with a better resolution.

Diffusion of the infrared radiation is probably a cause of the lack of correlation found in our study. It has been shown[67] that reflectance at 810 nm of dark-pigmented fundi and light-pigmented fundi did not strongly differ. This suggests that the reason why such reflectance measurements failed to provide us with useful information on the absorbing structures in the eye fundus stems from the poor sensitivity of such measurements to absorption changes due to the strong scattering properties of these tissues. Although large and highly pigmented choroidal structures are easily seen, small physiological choroidal pigmentation changes cannot be detected. This could contribute to "blurring" the images and reducing the detectability of deep-seated absorbing centers. This hypothesis is supported by many publications where the imaging of the choroid was found to be difficult, even with more sophisticated techniques.[67,80,81,100]

The choroidal blood flow is known to have an effect on the cooling down process. However,in thermal irradiations, this tissue cooling effect is only significant for long therapies ($>$10 s).[24,101–103] Variations in choroidal thickness and in the spatial distribution of the melanocytes probably play an important role in retinal burns: if the IR radiation is absorbed by the RPE and the choroid, then the heat deposited in these absorbing centers must diffuse down to the neuronal layer to create a retinal burn; the longitudinal location of the melanocytes may thus exert a significant influence on the tissue reaction.[104] Also, the resulting heating effect may notably change in function of the chorio-retinal thickness and the presence of exudate. Finally, it is quite possible that diseased eyes such as the ones studied in this paper undergo significant variations of retinal thickness, especially since it is also known that even healthy eyes undergo diurnal variations of choroidal thickness.[105]

Recent setups, still at the research stage, can produce contrasted images of the choroidal structures,[106–108] with a much better resolution than that of our fundus camera. At a wavelength of 810 nm, the latter had an estimated resolution in the order of $\approx$100 μm for structures at the surface of the retina, dropping to maybe $\approx$300 μm for structures deeper into the choroidal tissue.

Another interesting approach, relying on the measurement of the longitudinal reflectance profile (i.e., OCT A-scan) of the laser spot during irradiation, was proposed by Lanzetta and Dorin,[109] and Lanzetta et al.[27] It enables the detection of reflectance variations of specific layers within the fundus. This approach could allow, for example, monitoring of the reflectance of Bruch's membrane, and use of this measurement to modulate the laser irradiation duration, to prevent the formation of visible retinal burns.[103]

More generally, our study points toward a complex correlation between retinal optical parameters and retinal burns. It is unlikely that this correlation be governed by one parameter only, a conclusion that our study demonstrates. Our detection approach is set-up to mainly detect changes in pigmentation, and this parameter must have an impact on the occurrence of retinal burns, but our study shows that it is not the only one having an impact.

In spite of the not entirely conclusive nature of our results, our study opens the door for subsequent investigations. The subthreshold protocols, despite their proven efficiency to treat various

conditions, must be refined to avoid retinal burns, while allowing treatment in the upper end of the subthreshold regime. This was the rationale for the study we present here and it remains valid. It remains to be investigated if this method could be used in a different manner (other wavelength? several wavelengths?) or if an altogether different method (derived form the methods used for other purposes[110]) could give a clear-cut answer.

Acknowledgments

This work was supported by the Swiss National Science Foundation (Grant No. 205320-116556) and funded in part by the J. Jacobi Trust.

References

1. G. A. Moo-Young, "Lasers in ophthalmology," *High Tech Medicine [Special Issue] West J Med.* **143**(6), 745–750 (1985).
2. M. B. Parodi, G. Virgili, and J. R. Evans, "Laser treatment of drusen to prevent progression to advanced age-related macular degeneration," *Cochrane Database Syst. Rev. 1* CD006537 (2009).
3. J. S. Pollack et al., "Tissue effects of subclinical diode laser treatment of the retina," *Arch. Ophthalmol.* **116**(12), 1633–1639 (1998).
4. F. Ricci et al., "Indocyanine green enhanced subthreshold diode-laser micropulse photocoagulation treatment of chronic central serous chorioretinopathy," *Graefes Arch. Clin. Exp. Ophthalmol.* **247**(5), 597–607 (2009).
5. J. Roider, "Laser treatment of retinal diseases by subthreshold laser effects," *Semin. Ophthalmol.* **14**(1), 19–26 (1999).
6. S. H. Sarks et al., "Prophylactic perifoveal laser treatment of soft drusen," *Aust. N Z J. Ophthalmol.* **24**(1), 15–26 (1996).
7. M. Sculpher, "A preliminary economic evaluation of the diode laser in ophthalmology," *Lasers in Medical Science* **8**(3), 163–169 (1993).
8. D. V. Palanker, M. S. Blumenkranz, and M. F. Marmor, "Fifty years of ophthalmic laser therapy," *Arch. Ophthalmol.* **129**(12), 1613–1619 (2011).
9. D. V. Alfaro, *Age-Related Macular Degeneration: A Comprehensive Textbook*, 1st ed., Lippincott Williams & Wilkins, Philadelphia (2005).
10. M. S. Blumenkranz, "Optimal current and future treatments for diabetic macular oedema," *Eye* **24**, 428–434 (2010).
11. A. S. Banker and W. R. Freeman, "Retinal detachment," *Ophthalmol. Clin. North Am.* **14**(4), 695–704 (2001).
12. H. Y. Cho, Y. T. Kim, and S. W. Kang, "Laser photocoagulation as adjuvant therapy to surgery for large macular holes," *Korean J. Ophthalmol.* **20**(2), 93–98 (2006).
13. S. S. Hayreh, "Management of central retinal vein occlusion," *Ophthalmologica* **217**(3), 167–188 (2003).
14. Y. Takatsuna et al., "Long-term therapeutic efficacy of the subthreshold micropulse diode laser photocoagulation for diabetic macular edema," *Jpn. J. Ophthalmol.* **55**, 365–369 (2011).
15. B. P. Connolly et al., "The histopathologic effects of transpupillary thermotherapy in human eyes," *Ophthalmology* **110**(2), 415–420 (2003).
16. R. Parrozzani et al., "Long-term outcome of transpupillary thermotherapy as primary treatment of selected choroidal melanoma," *Acta. Ophthalmol.* **87**(7), 789–792 (2009).
17. M. Sickenberg, "Verteporfin therapy for subfoveal choroidal neovascularization in age-related macular degeneration: from clinical trials to clinical practice," *Semin. Ophthalmol.* **16**(4), 207–212 (2001).
18. H. van den Bergh, J. P. Ballini, and M. Sickenberg, "On the selectivity of photodynamic therapy of choroidal neovascularization associated with age-related macular degeneration," *J. Fr. Ophtalmol.* **27**(1), 75–78 (2004).
19. B. C. Wilson and M. S. Patterson, "The physics, biophysics and technology of photodynamic therapy," *Phys. Med. Biol.* **53**(9), 61–109 (2008).
20. Y. J. Hu, "Pain relief during panretinal photocoagulation for diabetic retinopathy," *Eye* **24**(8), 1416 (2010).
21. R. S. Kaiser et al., "One-year outcomes of panretinal photocoagulation in proliferative diabetic retinopathy," *Am. J. Ophthalmol.* **129**(2), 178–185 (2000).
22. A. L. McKenzie, "Physics of thermal processes in laser-tissue interaction," *Phys. Med. Biol.* **35**(9), 1175–1209 (1990).
23. Y. M. Paulus et al., "Healing of retinal photocoagulation lesions," *Invest. Ophthalmol. Vis. Sci.* **49**(12), 5540–5545 (2008).
24. M. A. Mainster, "Decreasing retinal photocoagulation damage: principles and techniques," *Semin. Ophthalmol.* **14**(4), 200–209 (1999).
25. J. W. Berger, "Thermal modeling of micropulsed diode laser retinal photocoagulation," *Lasers Surg. Med.* **20**(4), 409–415 (1997).
26. G. Dorin, "Subthreshold and micropulse diode laser photocoagulation," *Semin. Ophthalmol.* **18**(3), 147–153 (2003).
27. P. Lanzetta et al., "Theoretical bases of non-ophthalmoscopically visible endpoint photocoagulation," *Semin. Ophthalmol.* **16**(1), 8–11 (2001).
28. M. L. Laursen et al., "Subthreshold micropulse diode laser treatment in diabetic macular oedema," *Br. J. Ophthalmol.* **88**(9), 1173–1179 (2004).
29. C. M. Moorman and A. M. Hamilton, "Clinical applications of the micropulse diode laser," *Eye* **13**, 145–150 (1999).
30. G. Dorin, "Evolution of retinal laser therapy: minimum intensity photocoagulation (mip). Can the laser heal the retina without harming it?" *Semin. Ophthalmol.* **19**(1–2), 62–68 (2004).
31. D. Palanker et al., "The impact of pulse duration and burn grade on size of retinal photocoagulation lesion: implications for pattern density," *Retina* **31**(8), 1664–1669 (2011).
32. S. Sivaprasad et al., "Micropulsed diode laser therapy: evolution and clinical applications," *Survey of Ophthalmology* **55**(6), 516–530 (2010).
33. R. K. Banerjee et al., "Influence of laser parameters on selective retinal treatment using single-phase heat transfer analyses," *Med. Phys.* **34**(5), 1828–1841 (2007).
34. R. Brinkmann et al., "Origin of retinal pigment epithelium cell damage by pulsed laser irradiance in the nanosecond to microsecond time regimen," *Lasers Surg. Med.* **27**(5), 451–464 (2000).
35. R. Brinkmann, J. Roider, and R. Birngruber, "Selective retina therapy (srt): a review on methods, techniques, preclinical and first clinical results," *Bull. Soc. Belge. Ophtalmol.* **302**, 51–69 (2006).
36. C. Gustavsson and E. Agardh, "Transpupillary thermotherapy for occult subfoveal choroidal neovascularization: a 1-year, prospective randomized pilot study," *Acta. Ophthalmol. Scand.* **83**(2), 148–153 (2005).
37. Y. Ito et al., "Transpupillary thermotherapy: effect of wavelength on normal primate retina," *Retina* **25**(8), 1046–1053 (2005).
38. M. A. Mainster and E. Reichel, "Transpupillary thermotherapy for age-related macular degeneration: principles and techniques," *Semin. Ophthalmol.* **16**(2), 55–59 (2001).
39. R. S. Newsom et al., "Transpupillary thermotherapy (TTT) for the treatment of choroidal neovascularization," *Br. J. Ophthalmol.* **85**(2), 173–178 (2001).
40. P. Rol et al., "Transpupillar laser phototherapy for retinal and choroidal tumors: a rational approach," *Graefes Arch. Clin. Exp. Ophthalmol.* **238**(3), 249–272 (2000).
41. B. Stoffelns, "Transpupillary thermotherapy (TTT) for age-related macular degeneration (AMD)—Is it time to say good-bye?" *Med. Laser Appl.* **25**, 229–234 (2010).
42. R. W. Flower, "Optimizing treatment of choroidal neovascularization feeder vessels associated with age-related macular degeneration," *Am. J. Ophthalmol.* **134**(2), 228–239 (2002).
43. R. R. Margherio, A. R. Margherio, and M. E. DeSantis, "Laser treatments with verteporfin therapy and its potential impact on retinal practices," *Retina* **20**(4), 325–330 (2000).
44. M. F. Zuluaga et al., "Synergies of vegf inhibition and photodynamic therapy in the treatment of age-related macular degeneration," *Invest. Ophthalmol. Vis. Sci.* **48**(4), 1767–1772 (2007).
45. T. Sharma et al., "Transpupillary thermotherapy for circumscribed choroidal hemangioma: clinical profile and treatment outcome," *Ophthalmic Surg. Lasers Imaging* **42**(5), 360–368 (2011).
46. G. Io Giudice et al., "Large-spot subthreshold transpupillary thermotherapy for chronic serous macular detachment," *Clin. Ophthalmol.* **5**(1), 355–360 (2011).
47. T. J. Desmettre, C. A. Maurage, and S. Mordon, "Transpupillary thermotherapy (TTT) with short duration laser exposures induce heat

shock protein (hsp) hyperexpression on choroidoretinal layers," *Lasers Surg. Med.* **33**(2), 102–107 (2003).
48. J. M. Kim et al., "Thermal injury induces heat shock protein in the optic nerve head *in vivo*," *Invest. Ophthalmol. Vis. Sci.* **47**(11), 4888–4894 (2006).
49. M. A. Mainster and E. Reichel, "Transpupillary thermotherapy for age-related macular degeneration: long-pulse photocoagulation, apoptosis, and heat shock protein," *Ophthalmic Surg. Lasers* **31**(5), 359–373 (2000).
50. F. Piffaretti et al., "Hydrodynamic rebalancing laser therapy to treat age related macular degeneration: development of an instrumental setup to monitor this treatment using the retina reflectance at 810 nm," 2006, http://www.oculista-vezzola.it.
51. M. Sickenberg et al., "Incidence and fluorescence pharmacokinetic study of a temporal disc leak in wet age-related macular degeneration," (in preparation).
52. M. A. Mainster et al., "Retinal laser lenses: magnification, spot size, and field of view," *Br. J. Ophthalmol.* **74**(3), 177–179 (1990).
53. E. Vezzola and M. Sickenberg, private communication (2010).
54. C. J. Walter, "Disc leak in the pathogenesis of posterior retinal degenerations," *Aust. J. Ophthalmol.* **8**(3), 235–239 (1980).
55. F. Piffaretti et al., "Hydrodynamic rebalancing laser therapy to treat age-related macular degeneration," presented at *Biomedical Photonics Network Meeting*, Lausanne, Switzerland (2008).
56. J. Albon et al., "Age related compliance of the lamina cribrosa in human eyes," *Br. J. Ophthalmol.* **84**(3), 318–323 (2000).
57. D. G. Gomez et al., "Cerebrospinal fluid absorption in the rabbit optic pathways," *Graefes Arch. Clin. Exp. Ophthalmol.* **226**(1), 1–7 (1988).
58. S. S. Hayreh, "Prevalent misconceptions about acute retinal vascular occlusive disorders," *Prog. Retin. Eye Res.* **24**(4), 493–519 (2005).
59. A. Kotecha, S. Izadi, and G. Jeffery, "Age-related changes in the thickness of the human lamina cribrosa," *Br. J. Ophthalmol.* **90**(12), 1531–1534 (2006).
60. D. J. Moore, A. A. Hussain, and J. Marshall, "Age-related variation in the hydraulic conductivity of Bruch's membrane," *Invest. Ophthalmol. Vis. Sci.* **36**(7), 1290–1297 (1995).
61. A. Alm and A. Bill, "Ocular and optic nerve blood flow at normal and increased intraocular pressures in monkeys (macaca irus): a study with radioactively labeled microspheres including flow determinations in brain and some other tissues," *Exp. Eye Res.* **15**(1), 15–29 (1973).
62. E. Friedman et al., "Increased scleral rigidity and age-related macular degeneration," *Ophthalmology* **96**(1), 104–108 (1989).
63. I. G. Pallikaris et al., "Ocular rigidity in patients with age-related macular degeneration," *Am. J. Ophthalmol.* **141**(4), 611–615 (2006).
64. R. L. Radius and D. R. Anderson, "Breakdown of the normal optic nerve head blood-brain barrier following acute elevation of intraocular pressure in experimental animals," *Invest. Ophthalmol. Vis. Sci.* **19**(3), 244–255 (1980).
65. R. S. Ramrattan et al., "Morphometric analysis of Bruch's membrane, the choriocapillaris, and the choroid in aging," *Invest. Ophthalmol. Vis. Sci.* **35**(6), 2857–2864 (1994).
66. M. Sickenberg, personal communication (2010).
67. A. E. Elsner et al., "Infrared imaging of sub-retinal structures in the human ocular fundus," *Vision Res.* **36**(1), 191–205 (1996).
68. T. T. J. M. Berendschot, P. J. DeLint, and D. van Norren, "Fundus reflectance—historical and present ideas," *Prog. Retin. Eye Res.* **22**(2), 171–200 (2003).
69. F. C. Delori and K. P. Pflibsen, "Spectral reflectance of the human ocular fundus," *Appl. Opt.* **28**(6), 17 (1989).
70. M. R. Jerath et al., "Calibrated real-time control of lesion size based on reflectance images," *Appl. Opt.* **32**(7), 1200–1209 (1993).
71. C. N. Keilhauer and F. C. Delori, "Near-infrared autofluorescence imaging of the fundus: visualization of ocular melanin," *Invest. Ophthalmol. Vis. Sci.* **47**(8), 3556–3564 (2006).
72. J. Sandeau et al., "Numerical modeling of conductive and convective heat transfers in retinal laser applications," *J. Biophotonics* **1**(1), 43–52 (2008).
73. F. Viola et al., "Choroidal abnormalities detected by near-infrared reflectance imaging as a new diagnostic criterion for neurofibromatosis," *Ophthalmology* **119**(2), 369–375 (2012).
74. P. Nataliya et al., "Digital imaging of the fundus with long-wave illumination," *Klinika Oczna.* **111**(1–3) 18–20 (2009).
75. P. W. de Graaf, S. F. Barrett, and C. H. Wright, "A method to control irradiation time for laser photocoagulation of the retina—Part II," *Biomed. Sci. Instrum.* **35**, 159–163 (1999).
76. D. A. Ludwig, S. F. Barrett, and R. F. Kubichek, "Laser dosimetry control for retinal surgery," *Biomed. Sci. Instrum.* **37**, 479–484 (2001).
77. E. Naess et al., "Computer-assisted laser photocoagulation of the retina—a hybrid tracking approach," *J. Biomed. Opt.* **7**(2), 179–189 (2002).
78. M. Sickenberg and E. Vezzola, Save Sight Foundation, private communication (2010).
79. P. Thévenaz, U. E. Ruttimann, and M. Unser, "A pyramid approach to subpixel registration based on intensity," *IEEE Trans. Image Process.* **7**(1), 27–41 (1998).
80. E. M. Brezinski, "Optical coherence tomography theory," in *Optical Coherence Tomography*, pp. 97–145, Academic Press, Burlington (2006).
81. P. F. Sharp and A. Manivannan, "The scanning laser ophthalmoscope," *Phys. Med. Biol.* **42**(5), 951–966 (1997).
82. T. T. J. M. Berendschot and D. van Norren, "Objective determination of the macular pigment optical density using fundus reflectance spectroscopy," *Arch. Biochem. Biophys.* **430**(2), 149–155 (2004).
83. L. J. Bour et al., "Fundus photography for measurement of macular pigment density distribution in children," *Invest. Ophthalmol. Vis. Sci.* **43**(5), 1450–1455 (2002).
84. K. R. Denninghoff et al., "Blue-green spectral minimum correlates with oxyhemoglobin saturation *in vivo*," *J. Biomed. Opt.* **13**(5), 54–59 (2008).
85. S. Yoneya et al., "Retinal oxygen saturation levels in patients with central retinal vein occlusion," *Ophthalmology* **109**(8), 1521–1526 (2002).
86. S. F. Barrett et al., "Development of an integrated automated retinal surgical laser system," *Biomed. Sci. Instrum.* **32**, 215–224 (1996).
87. R. Birngruber, V. P. Gabel, and F. Hillenkamp, "Fundus reflectometry: a step towards optimization of the retina photocoagulation," *Mod. Probl. Ophthalmol.* **18**, 383–390 (1977).
88. M. S. Blumenkranz et al., "Semiautomated patterned scanning laser for retinal photocoagulation," *Retina* **26**(3), 370–376 (2006).
89. K. P. Pflibsen et al., "Fundus reflectometry for photocoagulation dosimetry," *App. Opt.* **28**(6), 1084–1096 (1989).
90. M. W. Ulbig, D. A. McHugh, and A. M. Hamilton, "Photocoagulation of choroidal neovascular membranes with a diode laser," *Br. J. Ophthalmol.* **77**(4), 218–221 (1993).
91. T. J. van den Berg and H. Spekreijse, "Near infrared light absorption in the human eye media," *Vision Res.* **37**(2), 249–253 (1997).
92. M. W. Balles et al., "Semiconductor diode laser photocoagulation in retinal vascular disease," *Ophthalmology* **97**(11), 1553–1561 (1990).
93. V. P. Gabel, R. Birngruber, and F. Hillenkamp, "Visible and near infrared light absorption in pigment epithelium and choroid," *Exerpta Med. Int. Congr.* **14**, 658–662 (1978).
94. P. Lanzetta, G. Virgili, and U. Menchini, "Diode laser photocoagulation of choroidal neovascular membranes," *Int. Ophthalmol.* **19**(6), 347–354 (1996).
95. R. Brancato et al., "Histopathology of diode and argon laser lesions in rabbit retina: a comparative study," *Invest. Ophthalmol. Vis. Sci.* **30**(7), 1504–1510 (1989).
96. J. G. Journée-de Korver et al., "Histopathological findings in human choroidal melanomas after transpupillary thermotherapy," *Br. J. Ophthalmol.* **81**(3), 234–239 (1997).
97. E. M. Procaccini et al., "The effects of a diode laser (810 nm) on pigmented guinea-pig skin," *Lasers Med. Sci.* **16**(3), 171–175 (2001).
98. F. Fankhauser and S. Kwasniewska, "Clinical effects of the Nd:YAG laser operating in the photodisruptive and thermal modes: a review," *Ophthalmologica* **217**(1), 1–16 (2003).
99. B. J. Lund, "Laser retinal thermal damage threshold: impact of small-scale ocular motion," *J. Biomed. Opt.* **11**(6), 064033 (2006).
100. H. Hammer et al., "Scattering properties of the retina and the choroids determined from oct-a-scans," *Int. Ophthalmol.* **23**(4–6), 291–295 (2001).
101. T. J. Desmettre et al., "Diode laser-induced thermal damage evaluation on the retina with a liposome dye system," *Lasers Surg. Med.* **24**(1), 61–68 (1999).
102. M. S. Ibarra et al., "Retinal temperature increase during transpupillary thermotherapy: effects of pigmentation, subretinal blood, and

choroidal blood flow," *Invest. Ophthalmol. Vis. Sci.* **45**(10), 3678–3682 (2004).
103. M. A. Mainster and D. H. Sliney, "TTT: local light absorption and heat convection versus heat conduction," *Br. J. Ophthalmol.* **89**(11), 1545 (2005).
104. R. F. Spaide, H. Koizumi, and M. C. Pozzoni, "Enhanced depth imaging spectral-domain optical coherence tomography," *Am. J. Ophthalmol.* **146**(4), 496–500 (2008).
105. C. S. Tan et al., "Diurnal variation of choroidal thickness in normal, healthy subjects measured by spectral domain optical coherence tomography," *Invest. Ophthalmol. Vis. Sci.* **53**(1), 261–266 (2012).
106. T. Fujiwara et al., "Enhanced depth imaging optical coherence tomography of the choroid in highly myopic eyes," *Am. J. Ophthalmol.* **148**(3), 445–450 (2009).
107. B. Povazay et al., "Wide-field optical coherence tomography of the choroid *in vivo*," *Invest. Ophthalmol. Vis. Sci.* **50**(4), 1856–1863 (2009).
108. D. van Norren and J. van de Kraats, "Imaging retinal densitometry with a confocal scanning laser ophthalmoscope," *Vision Res.* **29**(12), 1825–1830 (1989).
109. P. Lanzetta and G. Dorin, "Method and apparatus for real-time detection, control and recording of sub-clinical therapeutic laser lesions during ocular laser photocoagulation," Italy Patent No. 01932680.0-2305-US0113559 (2001).
110. A. A. Fawzi et al., "Recovery of macular pigment spectrum *in vivo* using hyperspectral image analysis," *J. Biomed. Opt.* **16**(10), 106008 (2011).